Geophysical Prospecting, 1997, **45**, 479–512

Moveout analysis for tranversely isotropic media with a tilted symmetry axis[1]

Ilya Tsvankin[2]

Abstract

The transversely isotropic (TI) model with a tilted axis of symmetry may be typical, for instance, for sediments near the flanks of salt domes. This work is devoted to an analysis of reflection moveout from horizontal and dipping reflectors in the symmetry plane of TI media that contains the symmetry axis. While for vertical and horizontal transverse isotropy zero-offset reflections exist for the full range of dips up to 90°, this is no longer the case for intermediate axis orientations. For typical homogeneous models with a symmetry axis tilted towards the reflector, wavefront distortions make it impossible to generate specular zero-offset reflected rays from steep interfaces. The 'missing' dipping planes can be imaged only in vertically inhomogeneous media by using *turning* waves. These unusual phenomena may have serious implications in salt imaging.

In non-elliptical TI media, the tilt of the symmetry axis may have a drastic influence on normal-moveout (NMO) velocity from horizontal reflectors, as well as on the dependence of NMO velocity on the ray parameter p (the 'dip-moveout (DMO) signature'). The DMO signature retains the same character as for vertical transverse isotropy only for near-vertical and near-horizontal orientation of the symmetry axis. The behaviour of NMO velocity rapidly changes if the symmetry axis is tilted away from the vertical, with a tilt of $\pm 20°$ being almost sufficient to eliminate the influence of the anisotropy on the DMO signature. For larger tilt angles and typical positive values of the difference between the anisotropic parameters ϵ and δ, the NMO velocity increases with p more slowly than in homogeneous isotropic media; a dependence usually caused by a vertical velocity gradient. Dip-moveout processing for a wide range of tilt angles requires application of anisotropic DMO algorithms.

The strong influence of the tilt angle on P-wave moveout can be used to constrain the tilt using P-wave NMO velocity in the plane that includes the symmetry axis. However, if the azimuth of the axis is unknown, the inversion for the axis orientation cannot be performed without a 3D analysis of reflection traveltimes on lines with different azimuthal directions.

---

[1] Received August 1995, revision accepted August 1996.

[2] Center for Wave Phenomena, Department of Geophysics, Colorado School of Mines, Golden, Colorado 80401-1887, USA.

Introduction

The behaviour of reflection moveout is of primary importance to most seismic processing steps, such as velocity analysis, normal-moveout (NMO) correction, dip-moveout (DMO) removal and migration. In seismic exploration, recording is conventionally carried out on common-midpoint (CMP) spreads with length comparable to the depth of the target horizon. For these moderate offset-to-depth ratios, P-wave reflection moveout is usually close to hyperbolic and is adequately described by the NMO velocity calculated in the zero-spread limit (Taner and Koehler 1969; Tsvankin and Thomsen 1994).

If the medium is anisotropic, NMO velocity is generally different from the root-mean-square (rms) vertical velocity. The influence of anisotropic parameters on NMO velocity has attracted considerable attention in the literature, but most existing work is restricted to a relatively simple (although common) model: transversely isotropic media with a vertical symmetry axis (VTI media). Several authors (e.g. Lyakhovitsky and Nevsky 1971), gave analytic expressions for NMO velocities of pure modes (P–P, SV–SV, SH–SH) from a horizontal reflector (the qualifiers in 'quasi-P-wave' and 'quasi-SV-wave' are omitted). For P-waves, the NMO velocity in a horizontal VTI layer depends only on the vertical velocity V_{P0} and the parameter δ introduced by Thomsen (1986),

$$V_{\mathrm{nmo}}[\text{P-wave}] = V_{P0}\sqrt{1+2\delta}. \tag{1}$$

Hake, Helbig and Mesdag (1984) showed that NMO velocity in layered VTI media is equal to the rms of the interval NMO velocities in the individual layers; they also presented the corresponding equations for the quartic moveout term of pure modes. NMO velocity in effective homogeneous VTI models formed by interbedding of thin isotropic layers was studied numerically by Levin (1979). Banik (1984) demonstrated on North Sea data that the deviation of the P-wave moveout velocity from the rms vertical velocity in anisotropic media may lead to substantial errors in time-to-depth conversion. NMO velocity for converted P–SV waves was expressed in terms of the moveout velocities of P–P and SV–SV waves by Seriff and Sriram (1991). Tsvankin and Thomsen (1994) gave an analytic description of long-spread (non-hyperbolic) reflection moveout of pure and converted waves in horizontally stratified VTI media; their treatment can be extended to symmetry planes of any anisotropic medium.

Anisotropy distorts not only the moveout in horizontally layered media, but also the NMO velocity for dipping reflectors. In isotropic, homogeneous media, the dip dependence of NMO velocity in the dip plane of the reflector is given by (Levin 1971)

$$V_{\mathrm{nmo}}(\phi) = \frac{V_{\mathrm{nmo}}(0)}{\cos\phi}, \tag{2}$$

where ϕ is the dip angle. Deviations from the cosine-of-dip dependence are of primary importance in DMO processing, as well as in the inversion for the anisotropic parameters. Analytic expressions for the dip-dependent NMO velocity in elliptically

anisotropic media were presented by Byun (1982) and Uren, Gardner and McDonald (1990). However, elliptical models are no more than a subset of transversely isotropic media that is not typical for subsurface formations (Thomsen 1986). Levin (1990) carried out a numerical study of the P-wave NMO velocities for dipping reflectors beneath homogeneous TI media and showed that there is no apparent correlation between the magnitude of velocity anisotropy and errors in the cosine-of-dip dependence. The same conclusion was drawn by Larner (1993) in his modelling study of the P-wave NMO velocities in VTI media with vertical-velocity gradient.

Tsvankin (1995) presented an equation for NMO velocity from dipping reflectors valid for pure modes in any symmetry plane in anisotropic media. He also transformed this exact equation into a much simpler expression for weakly anisotropic VTI media and gave an analytic explanation for the results of Levin (1990) and Larner (1993). Deviations from the cosine-of-dip dependence (equation (2)) in VTI media turned out to be primarily controlled by the *difference* between Thomsen's (1986) anisotropy parameters ϵ and δ. Alkhalifah and Tsvankin (1995) used the moveout equation of Tsvankin (1995) to study NMO velocity for dipping reflectors as a function of the ray parameter p, a quantity that is easier to obtain from reflection data than dip. They showed that for P-waves in VTI media, normal-moveout velocity from dipping reflectors is controlled by just two parameters: the zero-dip NMO velocity $V_{\mathrm{nmo}}(0)$ (defined in (1)) and an anisotropic parameter η, specified as

$$\eta \equiv \frac{\epsilon - \delta}{1 + 2\delta}. \tag{3}$$

They also proved that in VTI media the parameters V_{nmo} (0) and η are sufficient to perform all time-related processing steps, such as NMO correction, dip-moveout (DMO) removal, prestack and poststack time migration. Both parameters can be reliably recovered from P-wave surface data using NMO velocities and ray parameters measured for two different dips. Alkhalifah and Tsvankin (1995) also generalized the Dix (1955) NMO equation to models consisting of a stack of anisotropic horizontal layers above a dipping reflector. A more detailed overview of the moveout analysis in VTI media is given in Tsvankin (1996).

The papers mentioned above are focused on the behaviour of NMO velocity in transversely isotropic media with a vertical symmetry axis. The only non-VTI (azimuthally anisotropic) model examined by Tsvankin (1995) is the one with an in-plane symmetry axis normal to the reflector; in this case, in agreement with the numerical results of Levin (1990), the isotropic cosine-of-dip dependence of NMO velocity remains entirely valid. Another type of azimuthal anisotropy discussed in the literature is TI media with a horizontal symmetry axis (Thomsen 1988; Sena 1991). Reflection moveout for horizontal transverse isotropy (HTI media) is described in detail in a separate paper (Tsvankin 1997).

Here, the NMO equation of Tsvankin (1995) is used to examine moveout velocity in homogeneous transversely isotropic media with a tilted axis of symmetry confined

to the incidence (sagittal) plane. The tilt of the symmetry axis leads to a rotation of the P-wave wavefront that may cause the disappearance of specular zero-offset reflections from steep interfaces. For the symmetry axis tilted at an arbitrary angle, the NMO velocity is studied both analytically and numerically with emphasis on implications for DMO processing and anisotropic inversion. The analysis shows that the zero-dip NMO velocity $V_{\rm nmo}(0)$ and the parameter η are sufficient to describe P-wave NMO velocity in only a limited range of tilt angles that includes near-vertical and near-horizontal orientations of the symmetry axis.

NMO velocity and anisotropic parameters for TI media

Normal-moveout velocity of pure modes in symmetry planes of any anisotropic homogeneous medium is given by (Tsvankin 1995)

$$V_{\rm nmo}(\phi) = \frac{V(\phi)}{\cos\phi}\frac{\sqrt{1+\dfrac{V''(\phi)}{V(\phi)}}}{1-\tan\phi\dfrac{V'(\phi)}{V(\phi)}}, \tag{4}$$

where V is the phase velocity as a function of the phase angle θ with the vertical and ϕ is the dip of the reflector. For (4) to be valid, the incidence plane should coincide with the dip plane of the reflector. This assumption makes the problem two-dimensional by eliminating out-of-plane components of phase- and group-velocity vectors of the reflected waves. The familiar cosine-of-dip dependence of NMO velocity in isotropic media (2) can be obtained from (4) by setting $V(\theta)$ equal to a constant.

If the medium is transversely isotropic (hexagonal), (4) can be applied in the vertical plane that contains the symmetry axis and, if the symmetry axis is horizontal, in the isotropy plane that is normal to the symmetry axis. For an arbitrary mutual orientation of the symmetry axis and the incidence plane in TI media, (4) can be used only under the assumption of weak azimuthal anisotropy. Here, our goal is to study the dependence of NMO velocity on the anisotropy parameters and reflector dip for TI media with a symmetry axis confined to the incidence plane. In order to cover all possible mutual orientations of the reflector normal and the symmetry axis, the tilt angle ν spans the range $-90° < \nu < 90°$, while the dip ϕ is restricted to positive angles $0° < \phi < 90°$. Thus, positive values of ν mean that the axis is tilted towards the reflector, while $\nu < 0$ corresponds to the axis tilted away from the reflector. In principle, negative tilt angles can be avoided by using the analogy between TI models with the symmetry-axis orientations differing by 90° (Tsvankin 1997). However, since application of this analogy requires replacing the original anisotropic coefficients by the parameters of the equivalent model, it will not be used in this work.

The transversely isotropic model will be described by the Thomsen (1986) parameters defined in the rotated coordinate system associated with the symmetry axis, i.e.

$$V_{P0} \equiv \sqrt{\frac{c_{33}^{(R)}}{\rho}}, \tag{5}$$

$$V_{S0} \equiv \sqrt{\frac{c_{44}^{(R)}}{\rho}}, \tag{6}$$

$$\epsilon \equiv \frac{c_{11}^{(R)} - c_{33}^{(R)}}{2c_{33}^{(R)}}, \tag{7}$$

$$\delta \equiv \frac{(c_{13}^{(R)} + c_{44}^{(R)})^2 - (c_{33}^{(R)} - c_{44}^{(R)})^2}{2c_{33}^{(R)}(c_{33}^{(R)} - c_{44}^{(R)})}, \tag{8}$$

$$\gamma \equiv \frac{c_{66}^{(R)} - c_{44}^{(R)}}{2c_{44}^{(R)}}, \tag{9}$$

where ρ is the density, and the elastic constants $c_{ij}^{(R)}$ correspond to the rotated coordinate frame with the x_3-axis pointing in the symmetry direction. V_{P0} and V_{S0} are the P-wave and S-wave velocities, respectively, along the (tilted) symmetry axis; the dimensionless anisotropic coefficients ϵ, δ and γ become zero in isotropic media. A detailed description of notation for transversely isotropic media is given by Tsvankin (1996).

P–SV propagation for vertical transverse isotropy is determined by four coefficients: V_{P0}, V_{S0}, ϵ, and δ. P-wave velocities and traveltimes in VTI media depend largely on V_{P0}, ϵ and δ, while the influence of the shear-wave velocity V_{S0} is practically negligible (Tsvankin and Thomsen 1994; Tsvankin 1996). Hence, for TI media with a tilted axis of symmetry, P-wave NMO velocity is determined by V_{P0}, ϵ, δ and the tilt angle ν.

In the special case of a horizontal axis of symmetry, velocities and polarizations in the plane that contains the symmetry axis can be described in terms of the stiffness coefficients by the same equations as for vertical transverse isotropy (Tsvankin 1997). Therefore, for HTI media it is possible to replace the generic Thomsen coefficients introduced above by the Thomsen parameters of the 'equivalent' VTI model. For arbitrary tilt angles, however, it is more convenient to use the generic Thomsen parameters defined with respect to the symmetry axis.

Existence of dipping events in TI media

Before studying the dip dependence of NMO velocity, we have to find out whether it is possible to record dipping events for the full range of dips in anisotropic models. The wavefront excited by a point source in homogeneous, isotropic media is spherical with the rays normal to the wavefront. This means that, for any dip from 0 to 90°, there

exists a section of the wavefront parallel to the reflector. This section generates the normal-incidence (zero-offset) reflection that will be recorded at the source location; similarly, there always exists a specular reflection for non-zero source–receiver offsets. For a vertical reflector that extends all the way to the surface, the raypaths of the reflected waves are horizontal, and the traveltimes in the CMP geometry are independent of offset, which implies that the NMO velocity becomes infinite. For any other dip in the range from 0 to 90°, NMO velocity has a finite value, which is corroborated by the cosine-of-dip dependence of NMO velocity in isotropic media (equation (2)).

Angular velocity variations in anisotropic media distort the shape of the wavefront and the angular distribution of the wavefront normals. Here, the dip dependence of NMO velocity is considered in the plane that contains the symmetry axis. For the special cases of vertical (VTI) and horizontal (HTI) orientations of the axis, we still have no 'gaps' in the dip coverage of reflection data. Since the phase- and group-velocity vectors coincide with each other in the vertical and horizontal directions, the wavefront contains the full range of phase angles, despite all wavefront distortions at oblique angles of incidence (possible cusps on SV-wave wavefronts are not discussed here). Also, as for isotropic media, NMO velocity in VTI and HTI models becomes infinite for a vertical reflector. Indeed, the denominator in (4) for NMO velocity can be represented as

$$D = \cos\phi\left(1 - \tan\phi\frac{V'(\phi)}{V(\phi)}\right) = \cos\phi - \sin\phi\frac{V'(\phi)}{V(\phi)}. \tag{10}$$

Since for both vertical and horizontal symmetry axes the derivative of phase velocity at $\phi = 90°$ becomes zero, the denominator D vanishes for a vertical reflector.

The situation becomes much more complicated if the symmetry axis is tilted (within the incidence plane) at an arbitrary angle. It is still true that the wavefront from a point source in a homogeneous anisotropic half-space contains the full 90° range of *group* (*ray*) angles in any quadrant, but not necessarily the full range of *phase* angles that determine the direction of the wavefront normal. As a result, for some anisotropic models there are no wavefront normals perpendicular to dipping reflectors within a certain range of dips and, therefore, no corresponding zero-offset and small-offset reflections. Of course, this argument is based on the geometrical-seismics approximation; even in the absence of a specular reflection, the seismogram at the source location will contain some reflected energy that does not travel along the geometrical raypath. However, unless the reflector is close to the source, we cannot expect this non-specular reflection energy to be significant.

Figure 1 shows a typical P-wavefront for a symmetry axis tilted towards the reflector. Due to the increase in the phase and group velocity from the symmetry axis towards the horizontal, the maximum angle between the wavefront normal and the vertical in the lower right quadrant is limited to $\theta_{\max}$, i.e. the value corresponding to the horizontal ray. There are no wavefront normals in the angular range $\theta_{\max} < \theta < 90°$ and, therefore, no specular zero-offset reflections for dips larger than $\phi_{\max} = \theta_{\max}$.

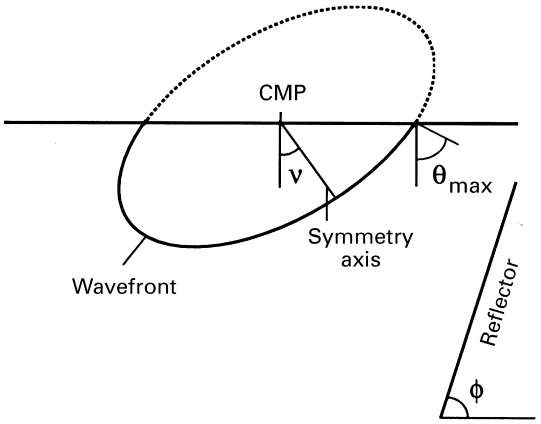

Figure 1. The P-wavefront for a transversely isotropic medium with a symmetry axis tilted towards the reflector. The increase in phase and group velocity away from the symmetry axis in this model reduces the angular range of the wavefront normals in the segment of the wavefront propagating towards the reflector. The maximum phase (wavefront) angle in the right lower quadrant is $\theta_{\max} < 90°$.

This schematic picture is substantiated by Fig. 2, which shows the results of anisotropic ray tracing (Rüger and Alkhalifah 1996) for a TI model with a steep reflector. Since the reflector dip in Fig. 2 exceeds $\phi_{\max}$, all the rays excited by the source propagate downwards after the reflection and cannot return to the surface. As a result, specular reflections do not exist even for non-zero offsets, and a CMP gather at the surface will not record *any* specular energy. Note that the tilt of the symmetry axis in

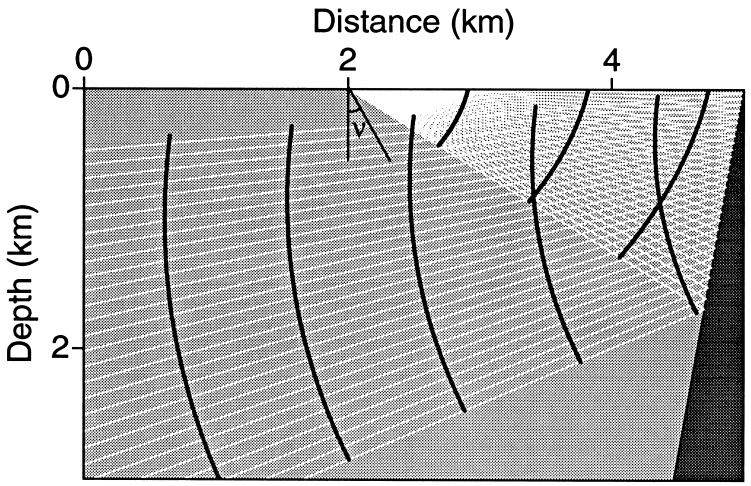

Figure 2. Rays (white) and wavefronts (black) of the P-wave excited by a point source at the surface and reflected from an interface dipping at 80°. The model parameters are $\nu = 20°$, $\epsilon = 0.25$, $\delta = 0.05$.

Fig. 2 is relatively mild (20°). The situation shown in Figs 1 and 2 may be typical for uptilted sediments (such as shales) near the flanks of salt domes because the direction normal to the bedding (and, hence, the expected symmetry axis of the TI medium) is tilted towards the salt body. In this case, we can expect serious problems in imaging of steep segments of the flanks, even if processing algorithms can handle transverse isotropy.

In order to find the maximum dip that would generate a specular reflection, let us express the group-velocity vector in the incidence (x,z)-plane through the phase velocity and phase angle (Berryman 1979):

$$\mathbf{V}_{\rm gr} = (V \sin\theta + V'(\theta)\cos\theta)\mathbf{x} + (V\cos\theta - V'(\theta)\sin\theta)\mathbf{z}. \tag{11}$$

The ray direction is horizontal if the vertical (z) component of group velocity is zero, i.e.

$$\cos\theta - \sin\theta\frac{V'(\theta)}{V(\theta)} = 0. \tag{12}$$

In the absence of cusps, (12) has two solutions (differing by $\pm 180°$) corresponding to the phase angle for the horizontal ray. For typical wavefronts with a monotonic change in the phase angle from the horizontal to the vertical ray, (12) determines the maximum phase angles for the two lower quadrants. Thus, we can use (12) to find the largest dip $\phi_{\rm max}$ for which we can record a specular reflection in the medium with the phase-velocity function $V(\theta)$ (assuming that the reflector starts at the surface).

In terms of the NMO velocity equation (4), the absence of phase angles corresponding to a certain range of dips results in zero and negative values of the denominator and, consequently, in infinite or non-existent NMO velocity. To understand the physical meaning of the denominator D (equation (10)), note that it becomes identical to the left-hand side of (12) if we substitute $\theta = \phi$. This implies that D vanishes if the zero-offset ray, which corresponds to the phase-velocity vector normal to the reflector, is horizontal (as for dip $\phi_{\rm max} = \theta_{\rm max}$ in Fig. 1). In other words, the NMO velocity becomes infinite if the zero-offset reflected ray (along with non-zero-offset rays) travels along the horizontal (common-midpoint) line. For larger dips, as explained above, specular reflections do not exist.

The magnitude of this unusual phenomenon is illustrated in Fig. 3 for a typical TI model with an increase in phase velocity away from the symmetry axis. Even a relatively mild tilt of 20–25° is sufficient to make it impossible to record zero-offset reflections for dips exceeding 76°. Note that the dependence of $\phi_{\rm max}$ on the tilt angle ν is asymmetric with respect to $\nu = 45°$. The dip $\phi_{\rm max}$ reaches its smallest value at tilt angles of 20–30° when the horizontal ray (responsible for $\phi_{\rm max}$) corresponds to the most distorted section of the wavefront, characterized by a rapid increase in phase velocity with angle. In contrast, at tilt angles $\nu > 50°$ the section of the wavefront close to the horizontal has a shape much closer to spherical (since the parameter δ, responsible for the P-wave phase velocity near the symmetry direction, is small), and the range of 'missing' dips is narrower.

Of course, a tilt of the symmetry axis towards the reflector does not cause the disappearance of steep dips for *all* TI models. In some TI media, phase velocity as a

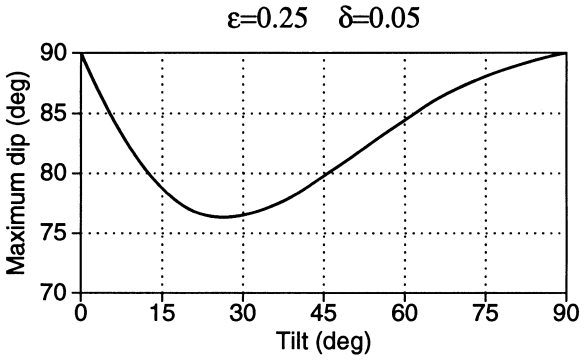

Figure 3. The dip $\phi_{\max}$ of the steepest reflector that generates a zero-offset P-wave ray for TI models with different tilt angles ν (calculated using (12)). The model is shown in Fig. 1; $\epsilon = 0.25$, $\delta = 0.05$.

function of phase angle with the symmetry axis decreases in certain angle ranges. If, due to the tilt of the axis, the horizontal ray direction corresponds to such a range, the wavefront moving towards the reflector contains all phase angles up to (and even beyond) 90°. For instance, this situation occurs for (less typical) models with large δ ($\delta \gg \epsilon$) and mild positive tilt angles.

An example of a wavefront containing the full range of phase angles in the quadrant of interest is shown in Fig. 4. Although the wavefront in Fig. 4 has the same shape as in Fig. 1, the symmetry axis is now tilted away from the reflector; we would have had the same situation in Fig. 1 had the reflector been located to the *left* of the source. For the

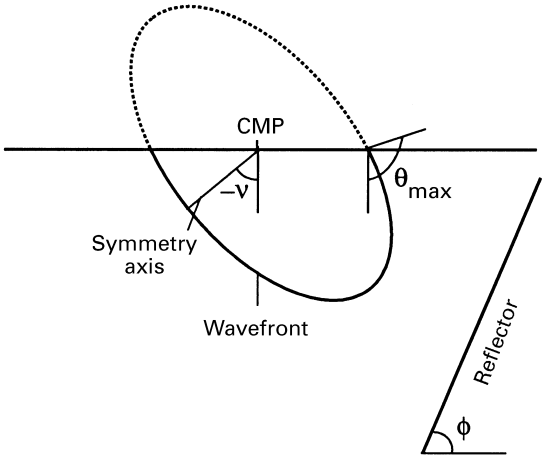

Figure 4. The wavefront for the same TI medium as in Fig. 1 but with a symmetry axis tilted away from the reflector. The direction of the wavefront normal in the lower right quadrant not only spans the full 0–90° range but also includes angles beyond 90°. The angle ν between the symmetry axis and vertical is taken to be negative if the symmetry axis is tilted away from the reflector.

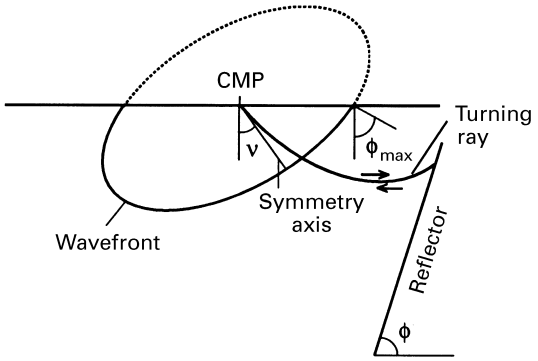

Figure 5. Reflections from steep interfaces in a factorized TI medium with constant ϵ and δ and an increase in the vertical velocity with depth. The shape of the wavefront at any depth is the same as in Fig. 1. In this case, specular zero-offset reflections from steep dips with $\phi_{max} > \theta_{max}$ represent turning rays.

case displayed in Fig. 4, the phase-velocity vector of the horizontal ray (ϕ_{max} is a solution of (12)) points upwards, and it is possible to record specular reflections not only from any dip in the 0–90° range, but also for dips between 90° and ϕ_{max}, if the aperture is sufficient. We conclude that anisotropy can make it possible to record reflections from overhang structures even in the absence of a velocity gradient.

In the above discussion we assumed a homogeneous anisotropic medium. Some of our conclusions can be extended in a straightforward way to the so-called factorized anisotropic media (e.g. Larner 1993) with a vertical velocity gradient. In factorized models the ratios of the elastic constants (and Thomsen's (1986) anisotropy parameters) are independent of spatial position and, consequently, the shape of the slowness surface and the relationship between the phase and group velocities remains the same throughout the medium. As a result, for factorized TI media with the same shape of the slowness surface as for the model in Fig. 1, the downgoing wavefield in the lower right quadrant still cannot contain phase (wavefront) angles exceeding θ_{max} (Fig. 5). However, the upgoing wavefield formed due to the ray bending does include the missing phase angles in the range $\theta_{max} < \theta < 90°$, as well as phase angles beyond 90°. Therefore, in such a medium, zero-offset reflections for dips $\phi_{max} < \phi < 90°$ ($\phi_{max} = \theta_{max}$) represent *turning* rays that exist only for appropriate spatial positions of the reflector with respect to the source.

NMO velocity as a function of dip angle

The behaviour of normal-moveout velocity for all three modes (P, SV, SH) is examined here for homogeneous TI media with a tilted in-plane axis of symmetry. It should be mentioned that, in the presence of non-elliptical anisotropy, reflection moveout is non-hyperbolic even for a homogeneous medium above the reflector. Therefore, although (4) can be applied for any tilt angle and any strength of the anisotropy, NMO velocity

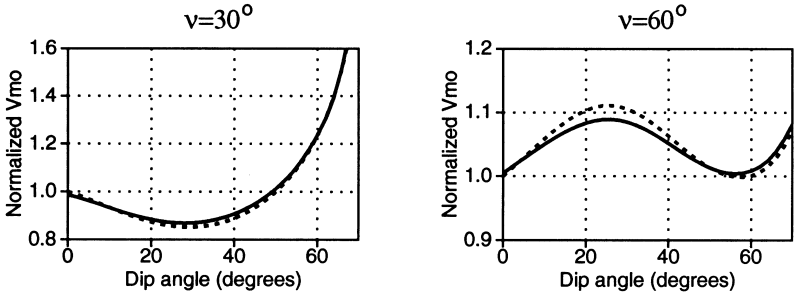

Figure 6. The influence of non-hyperbolic moveout on P-wave moveout velocity for a model with $\epsilon = 0.2$ and $\delta = 0.03$ and two tilt angles ($\nu = 30°$ and $\nu = 60°$). The solid curve is the effective moveout velocity calculated from the exact traveltimes (obtained by ray tracing) on the spreadlength equal to the distance between the CMP and the reflector; the dotted curve is the exact NMO velocity computed from (4). Both curves are normalized by $V_{\mathrm{nmo}}(0)/\cos\phi$, where $V_{\mathrm{nmo}}(0)$ is the exact NMO velocity for a horizontal reflector.

itself describes only the hyperbolic (short-spread) portion of the moveout curve. Due to the influence of non-hyperbolic moveout, stacking (moveout) velocity determined on finite spreads may deviate from the 'zero-spread' value given by (4). Studies of non-hyperbolic moveout for vertical transverse isotropy have shown, however, that for conventional spreadlengths comparable to the CMP-reflector distance, the magnitude of anisotropy-induced P-wave non-hyperbolic moveout is small and, moreover, decreases with reflector dip (Tsvankin and Thomsen 1994; Tsvankin 1995). Figure 6 demonstrates that this conclusion remains valid in TI media with a *tilted* symmetry axis as well. The finite-spread moveout (stacking) velocity in Fig. 6 was calculated by fitting a straight line to the exact traveltimes ($t^2 - x^2$ curves) over a spread equal to the distance between the CMP and reflector. Evidently, despite the pronounced anellipticity of the TI model used in Fig. 6 ($\epsilon - \delta = 0.17$), the finite-spread moveout velocity is close to the analytic NMO value for the whole range of dips. Therefore, NMO velocity from (4) provides a sufficiently accurate description of P-wave reflection moveout for commonly used spreadlength-to-depth ratios. In principle, the non-hyperbolic moveout equation of Tsvankin and Thomsen (1994) can be extended to TI models with a tilted in-plane axis of symmetry, but analysis of non-hyperbolic moveout is outside the scope of this paper.

The results of Tsvankin (1995) indicate noticeable differences in the dependence of NMO velocity in VTI media on dip as opposed to ray parameter. Although for the purposes of seismic processing it is more convenient to use the ray parameter as the argument, the dependence of NMO velocity on the dip still deserves a separate discussion. The special case of elliptical anisotropy, which is relatively easy to treat analytically, is considered first. Then, the NMO equation for general (non-elliptical) transverse isotropy with the axis of symmetry rotated at an arbitrary angle is simplified by means of the weak-anisotropy approximation. Comparison of the weak-anisotropy and exact numerical results elucidates the dip dependence of NMO velocity for a representative range of homogeneous TI models with a tilted symmetry axis.

Elliptical anisotropy

Transverse isotropy always means elliptical anisotropy for the SH-wave, while, for P–SV-waves, elliptical media represent only the subset of TI models that satisfy the condition $\epsilon = \delta$. Although existing data indicate that elliptical anisotropy is not typical for TI formations, such as shales (Thomsen 1986; Sayers 1994), it is still instructive to examine this special case separately.

As shown in Appendix A, the NMO velocity for P-waves in elliptical media with tilted elliptical axes is given by

$$V_{\rm nmo}(\phi) = \frac{V_{\rm P0}}{\cos\phi}\sqrt{1+2\delta}\sqrt{1+2\delta\sin^2(\phi-\nu)}\left[1-2\delta\frac{\sin\nu\sin(\phi-\nu)}{\cos\phi}\right]^{-1}. \tag{13}$$

Equation (13) coincides with the normal-moveout equation of Uren *et al.* (1990) obtained using a different approach and presented in a different notation.

For a vertical symmetry axis ($\nu = 0$), (13) reduces to the expression discussed by Tsvankin (1995):

$$V_{\rm nmo}(\phi) = \frac{V_{\rm P0}\sqrt{1+2\delta}\sqrt{1+2\delta\sin^2\phi}}{\cos\phi}. \tag{14}$$

Equation (14) can be rewritten as

$$\frac{V_{\rm nmo}(\phi)\cos\phi}{V_{\rm nmo}(0)} = \frac{V_{\rm P}(\phi)}{V_{\rm P0}}, \tag{15}$$

where $V_{\rm P}$ is the P-wave phase velocity. Equation (15) shows that if the elliptical axes are not tilted, the error in the cosine-of-dip dependence is determined directly by the phase-velocity variations.

If the reflector is horizontal ($\phi = 0$), (13) reduces to

$$V_{\rm nmo}(0) = V_{\rm P0}\frac{\sqrt{1+2\delta}}{\sqrt{1+2\delta\sin^2\nu}} = V_{\rm P0}\sqrt{1+\frac{2\delta\cos^2\nu}{1+2\delta\sin^2\nu}}. \tag{16}$$

Let us compare the NMO velocity from (16) with the horizontal phase velocity

$$V_{\rm hor} = V_{\rm P0}\sqrt{1+2\delta\cos^2\nu}. \tag{17}$$

Equations (16) and (17) confirm the well-known fact that for a model with a vertical (or horizontal) elliptical axis ($\nu = 0^\circ$ or $\nu = 90^\circ$), the NMO velocity from a horizontal reflector is equal to the horizontal velocity. Although this is no longer strictly true for elliptical models with tilted axes, the difference between the two velocities is small since they coincide in the weak-anisotropy approximation. Indeed, for weak anisotropy ($|\delta| \ll 1$) we can drop the terms quadratic in δ, and then

$$V_{\rm nmo}(0) = V_{\rm P0}(1+\delta\cos^2\nu) = V_{\rm hor}. \tag{18}$$

Thus, in elliptical media, the NMO velocity from a horizontal reflector remains close to the horizontal phase velocity, whether the elliptical axes are tilted or not.

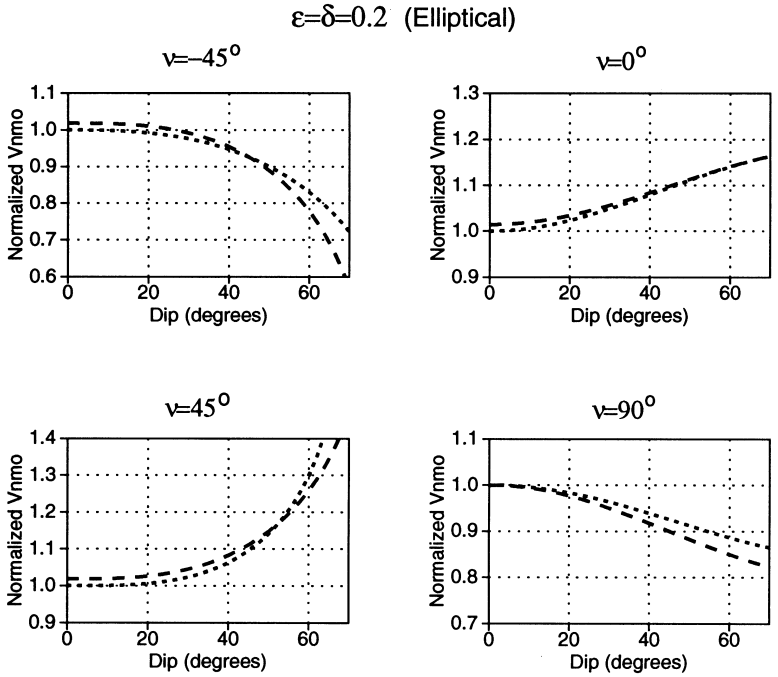

Figure 7. The dip dependence of P-wave moveout velocity for elliptical anisotropy ($\epsilon = \delta = 0.02$). The dotted curve is the exact NMO velocity calculated from (13); the dashed curve is the weak-anisotropy approximation from (19). Both curves are normalized by $V_{\rm nmo}(0)/\cos\phi$, where $V_{\rm nmo}(0)$ is the exact NMO velocity for a horizontal reflector.

Equation (13) for an arbitrary tilt of the symmetry axis can also be simplified under the assumption of weak anisotropy ($|\delta| \ll 1$):

$$V_{\rm nmo}(\phi) = \frac{V_{\rm P0}}{\cos\phi}\left[1 + \delta + \delta\sin^2(\phi - \nu) + 2\delta\frac{\sin\nu\sin(\phi - \nu)}{\cos\phi}\right]. \tag{19}$$

Figure 7 shows that the tilt has a significant impact on the dip dependence of NMO velocity in elliptical media. In order to separate the influence of the anisotropy, the curves in Fig. 7 are normalized by the isotropic equation (2). When one of the elliptical axes is vertical ($\nu = 0°$ or $\nu = 90°$), deviations from the cosine-of-dip relationship are entirely controlled by the phase-velocity variations (15). Although the difference between the vertical and horizontal velocities for the model in Fig. 7 is significant (close to 20%), the anisotropy-induced error in the cosine-of-dip relationship for both $\nu = 0$ and $\nu = 90°$ is relatively small. In contrast, for the symmetry axis tilted at 45° and −45°, the anisotropic signature is much more pronounced. Note that at $\nu = 45°$ the NMO velocity tends to infinity at dips below 90° since the section of the wavefront propagating towards the reflector does not contain the full range of the phase angles; this was discussed in detail in the previous section.

In general (non-elliptical) VTI media with $\epsilon \neq \delta$, equations for elliptical anisotropy are valid only for the SH-wave. Our moveout analysis for the elliptical P-wave remains entirely valid for the SH-wave if we replace V_{P0} with V_{S0} and δ with γ. For instance, the exact NMO velocity equation (13) for the SH-wave takes the form

$$V_{\rm nmo}(\phi)[\mathrm{SH}] = \frac{V_{S0}}{\cos\phi}\sqrt{1+2\gamma}\sqrt{1+2\gamma\sin^2(\phi-\nu)}\left[1-2\gamma\frac{\sin\nu\sin(\phi-\nu)}{\cos\phi}\right]^{-1}. \quad (20)$$

For SV-waves, the elliptical condition ($\epsilon = \delta$) implies that the phase and group velocities are independent of angle (however, SV-wave amplitudes can still be distorted by the anisotropy). Therefore, the NMO velocity for the SV-wave in elliptical media is described by the familiar isotropic cosine-of-dip dependence (2).

Weak transverse isotropy

The exact normal-moveout velocity (4) is too complex (especially when the symmetry axis is tilted) to separate the contributions of the anisotropy parameters to the NMO velocity. For the sake of qualitative moveout analysis, it is convenient to assume that the anisotropic coefficients are small and apply the weak-anisotropy approximation. The P-wave NMO velocity, linearized in the parameters ϵ and δ, is derived in Appendix B:

$$V_{\rm nmo}(\phi)\cos\phi = V_{P0}\left\{1+\delta+\delta\sin^2\bar{\phi}+3(\epsilon-\delta)\sin^2\bar{\phi}(2-\sin^2\bar{\phi}) + \frac{2\sin\nu\sin\bar{\phi}}{\cos\phi}[\delta+2(\epsilon-\delta)\sin^2\bar{\phi}]\right\}, \quad (21)$$

where $\bar{\phi} = \phi - \nu$.

For $\nu = 0$, (21) reduces to the expression given by Tsvankin (1995) for vertical transverse isotropy:

$$V_{\rm nmo}(\phi)\cos\phi = V_{P0}[1+\delta+\delta\sin^2\phi+3(\epsilon-\delta)\sin^2\phi(2-\sin^2\phi)]. \quad (22)$$

The terms on the first line of (21) have the same form as the VTI equation (22) but with the dip ϕ replaced by the difference $\phi - \nu$. The last term of (21) is a pure contribution of the tilt of the symmetry axis; note that it becomes zero not only for $\nu = 0$, but also when the dipping reflector is normal to the symmetry axis ($\bar{\phi} = 0$). In the latter case, all anisotropic angular terms in (21) vanish and the dip dependence of NMO velocity is described by the isotropic cosine-of-dip relationship (Levin 1990; Tsvankin 1995).

For a horizontal reflector ($\phi = 0$) and an arbitary tilt angle, the P-wave NMO velocity is given by

$$V_{\rm nmo}(0) = V_{P0}[1+\delta-\delta\sin^2\nu+(\epsilon-\delta)\sin^2\nu(7\cos^2\nu-1)]. \quad (23)$$

Equation (23) shows that the contribution of tilt to the expression for the NMO velocity from a horizontal reflector is mostly controlled by the difference $\epsilon - \delta$. The influence of tilt on the zero-dip NMO velocity (for models with fixed Thomsen parameters) is quite substantial and can change in a significant way the ratio of the NMO and vertical velocities, which is responsible for anisotropy-induced mis-ties in time-to-depth conversion. For example, for VTI media ($\nu = 0$), $V_{\rm nmo}(0) = V_{\rm P0}(1 + \delta)$, whereas for HTI media ($\nu = 90°$), $V_{\rm nmo}(0) = V_{\rm P0}(1 + \delta - \epsilon)$. However, the form of the expression for NMO velocity in HTI media becomes identical to that in VTI media (in the symmetry plane that contains the symmetry axis) if it is expressed through the stiffness coefficients or the Thomsen parameters of the 'equivalent' VTI model (Tsvankin 1997).

The ratio of the cosine-of-dip corrected NMO velocity (equation (21)) and the zero-dip value $V_{\rm nmo}(0)$ (equation (23)) determines the error in the dip dependence of NMO velocity caused by the anisotropy. The presence of a separate 'tilt' term in (21), as well as the form of the argument $(\phi - \nu)$ in other terms, is indicative of a strong influence of tilt on the dip dependence of the P-wave NMO velocity. Since the 'tilt' term depends on ϵ and δ separately, we can no longer expect that deviations from the cosine-of-dip dependence will be largely controlled by the difference between ϵ and δ, as was the case in VTI media. This conclusion is supported by the numerical results below.

To study the SV-wave NMO velocity, it is convenient to introduce the parameter σ (Tsvankin and Thomsen 1994):

$$\sigma \equiv \left(\frac{V_{\rm P0}}{V_{\rm S0}}\right)^2 (\epsilon - \delta). \tag{24}$$

The weak-anisotropy approximation for SV-waves can then be obtained from P-wave equation (21) by making the following substitutions (Tsvankin 1995): $V_{\rm P0} \rightarrow V_{\rm S0}$, $\delta \rightarrow \sigma$, and $\epsilon \rightarrow 0$, giving

$$V_{\rm nmo}(\phi)\cos\phi = V_{\rm S0}\left\{1 + \sigma + \sigma\sin^2\bar{\phi} - 3\sigma\sin^2\bar{\phi}(2 - \sin^2\bar{\phi}) + 2\sigma\frac{\sin\nu\sin\bar{\phi}\cos 2\bar{\phi}}{\cos\phi}\right\}. \tag{25}$$

As discussed above, for the SH-wave anisotropy is elliptical, and the NMO velocity is given exactly by (20).

Numerical results for general TI media

Figures 8 and 9 show the comparison between the exact P-wave NMO velocity (4) and the weak-anisotropy approximation (21) at different tilt angles for two media with small and moderate values of the anisotropic parameters ϵ and δ. For both models, as expected, the accuracy of the weak-anisotropy approximation is satisfactory at all tilt angles.

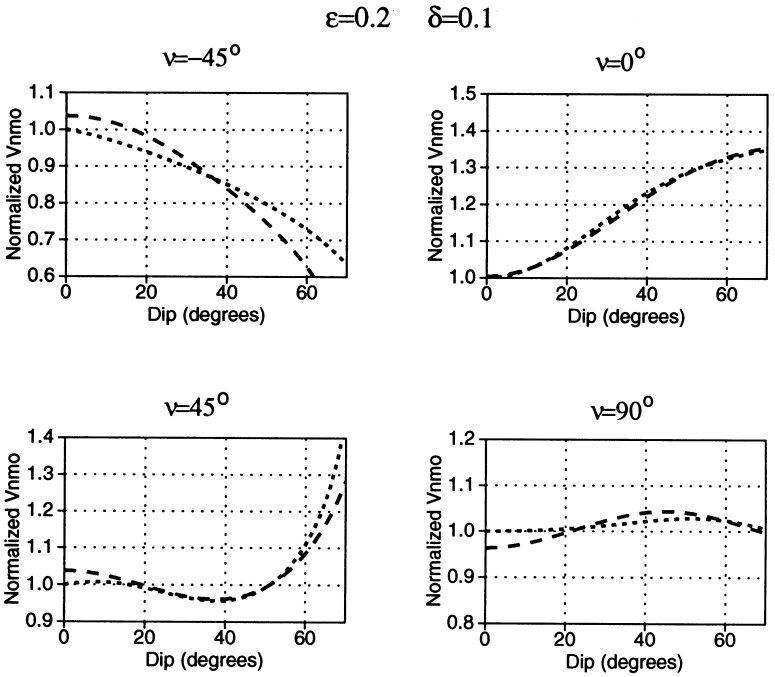

Figure 8. P-wave normal-moveout velocity for $\epsilon = 0.2$ and $\delta = 0.1$. The dotted curve is the exact NMO velocity calculated from (4); the dashed curve is the weak-anisotropy approximation from (21). Both curves are normalized by $V_{\rm nmo}(0)/\phi$, where $V_{\rm nmo}(0)$ is the exact NMO velocity for a horizontal reflector.

Clearly, the tilt of the symmetry axis has a strong influence on the behaviour of NMO velocity. It is interesting that for the model parameters used in Fig. 9, the NMO velocity is identical for $\nu = \pm 45°$, and also for $\nu = 0$ and $\nu = 90°$. This is explained by the vanishing parameter ϵ for this model: if $\epsilon = 0$, the P and SV phase velocities are symmetric with respect to the 45° angle with the symmetry axis. In this case the phase velocity and, consequently, the NMO velocity do not change when we rotate the symmetry axis by 90°.

Figures 8 and 9 also demonstrate that the character of the NMO-velocity curves is strongly dependent on the sign of $\epsilon - \delta$. For vertical transverse isotropy, the difference $\epsilon - \delta$ is believed to be predominantly positive, at least on the scale of seismic experiments (Thomsen 1986; Sayers 1994). The same is usually true for TI media where the anisotropy is due to a system of parallel cracks (Thomsen 1995). Note that $\epsilon - \delta > 0$ for transverse isotropy caused by the interbedding of thin parallel isotropic layers (Berryman 1979). Therefore, whether the tilt of the axis is caused by dipping TI formations (e.g. shales) or a system of oblique parallel cracks, typically $\epsilon - \delta > 0$.

Figure 10 illustrates the influence of tilt on the P-wave NMO velocity for three models with a positive $\epsilon - \delta = 0.2$. As predicted by the weak-anisotropy approximation, the tilt

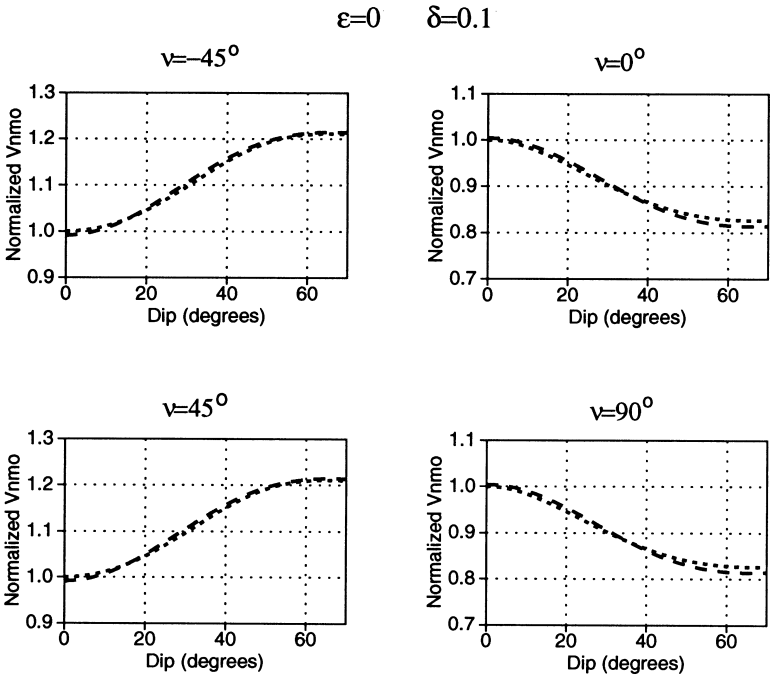

Figure 9. Normalized P-wave NMO velocity for $\epsilon = 0$ and $\delta = 0.1$. The dotted curve is the exact NMO velocity calculated from (4); the dashed curve is the weak-anisotropy approximation from (21).

causes profound changes in the character of the NMO curves. If the symmetry axis is tilted towards the reflector ($\nu > 0$), the cosine-of-dip corrected NMO velocity remains almost flat in the range $0 < \phi < \nu$ and then increases for steep dips. A 'negative' tilt $\nu < 0$, which corresponds to the symmetry axis tilted away from the reflector, reverses the NMO curve and makes the cosine-of-dip corrected NMO velocity decrease with dip. For a vertical symmetry axis, this type of behaviour arises for a negative value of $\epsilon - \delta$. Also, when the symmetry axis is tilted, the dip dependence of the P-wave NMO velocity is no longer tightly controlled by the difference $\epsilon - \delta$; the influence of the individual values of ϵ and δ is especially significant for a tilt of 45°.

Deviations of the P-wave NMO curves from those for vertical transverse isotropy become pronounced at relatively mild tilts (Fig. 11). Only for tilt angles up to $\pm(10 - 15)°$ is the dip dependence of NMO velocity close to that for VTI media. A tilt of $\pm 20°$ is sufficient to cause substantial changes in the NMO curves, with negative ν leading to a decrease in V_{nmo} with angle at steep dips. For $\nu = 20°$, the NMO velocity increases sharply at $\phi > 50°$ as the dip approaches the maximum phase angle $\phi_{\max}$ contained in the wavefront for this model (see the discussion above).

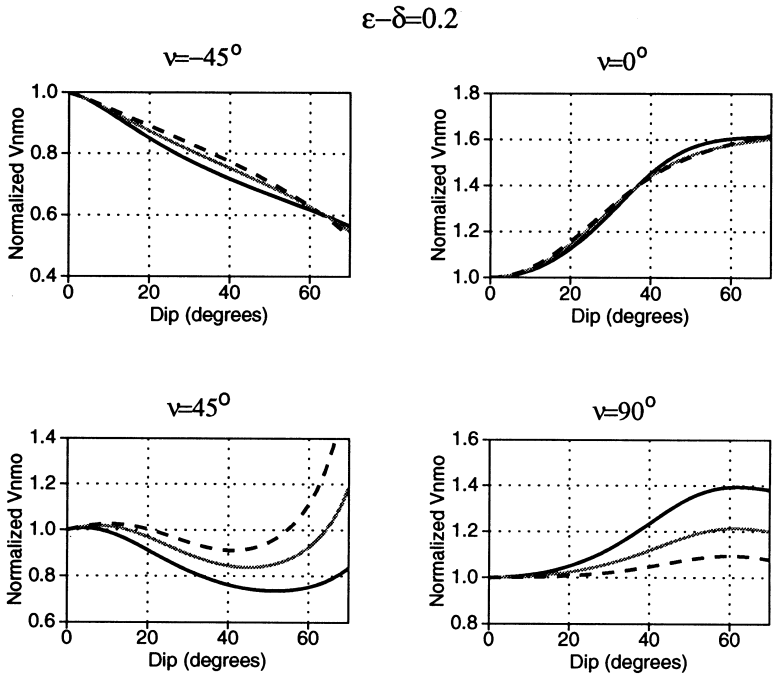

Figure 10. The exact normalized P-wave NMO velocity for models with $\epsilon - \delta = 0.2$: $\epsilon = 0.1$, $\delta = -0.1$ (solid black); $\epsilon = 0.2$, $\delta = 0$ (gray); $\epsilon = 0.3$, $\delta = 0.1$ (dashed).

NMO velocity as a function of ray parameter

Since reflection data do not carry explicit information about the dip angle, for application in seismic processing (4) should be rewritten as a function of the ray parameter $p(\phi)$ given by the slope of reflections on zero-offset (or CMP-stacked) seismic sections, i.e.

$$p(\phi) = \frac{1}{2}\frac{\mathrm{d}t_0}{\mathrm{d}x_0} = \frac{\sin\phi}{V(\phi)}, \tag{26}$$

where $t_0(x_0)$ is the two-way traveltime on the zero-offset (or stacked)section, and x_0 is the midpoint position. The dependence of NMO velocity (equation (4)) on the ray parameter is easy to find parametrically by using the dip ϕ as the argument.

First, consider $V_{\mathrm{nmo}}(p)$ for the simplest model wherein the anisotropy is elliptical. In the previous section it was demonstrated that the tilt of the elliptical axes has a significant influence on the dip dependence of NMO velocity. However, if represented through the ray parameter, the NMO velocity for elliptical anisotropy takes exactly the same form as in isotropic media (Appendix A):

$$V_{\mathrm{nmo}}(p) = \frac{V_{\mathrm{nmo}}(0)}{\sqrt{1 - p^2 V_{\mathrm{nmo}}^2(0)}}. \tag{27}$$

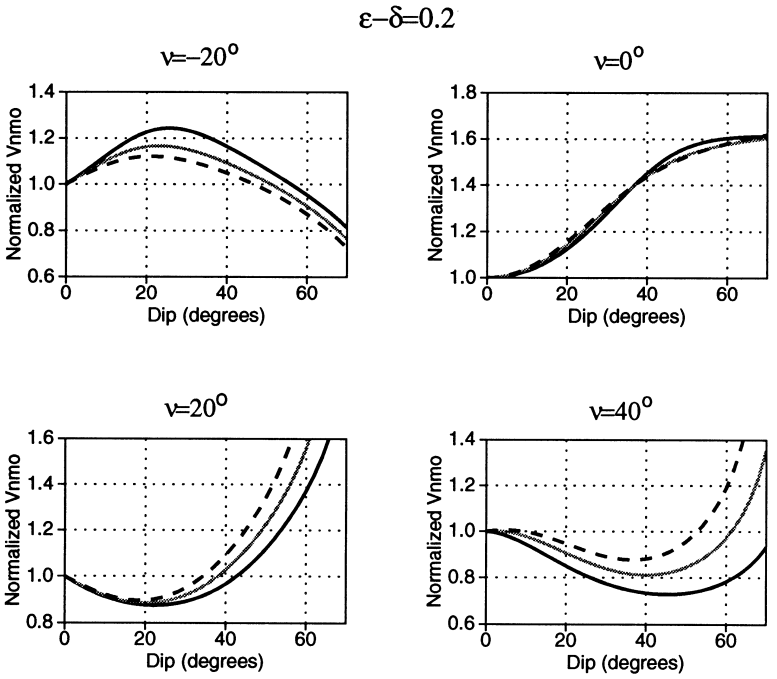

Figure 11. The exact normalized P-wave NMO velocity for mild tilt angles. The models are the same as in Fig. 10: $\epsilon = 0.1$, $\delta = -0.1$ (solid black); $\epsilon = 0.2$, $\delta = 0$ (gray); $\epsilon = 0.3$, $\delta = 0.1$ (dashed).

Given the complexity of $V_{\mathrm{nmo}}(\phi)$ in elliptically anisotropic models (13), it is somewhat surprising that the dependence of NMO velocity on the ray parameter remains 'isotropic' irrespective of the tilt of the elliptical axes. The contribution of anisotropy (including the tilt) in (27) is hidden in the values of the zero-dip NMO velocity $V_{\mathrm{nmo}}(0)$ (equation (16)) and the ray parameter p. Since the moveout for elliptical anisotropy with any orientation of the axes is purely hyperbolic (Uren *et al.* 1990), all isotropic time-related processing methods (NMO, DMO, time migration) are entirely valid in elliptical media. Note that this result has been proved by Helbig (1983) for the special case of the symmetry axis normal to the upper boundary of the layer of interest. The above conclusions (and (27)) are also fully applicable to the SH-wave in any TI media.

Equation (27) also implies that deviations from the isotropic $V_{\mathrm{nmo}}(p)$ dependence for *any tilt* should be strongly dependent on the difference $\epsilon - \delta$ which quantifies the degree of 'anellipticity' of TI media. It is clear, for instance, that the anisotropic term in the weak-anisotropy approximation for $V_{\mathrm{nmo}}(p)$ should contain ϵ and δ only in the combination $\epsilon - \delta$. Otherwise, this term would not vanish for elliptical anisotropy which corresponds to $\epsilon = \delta$.

Before analysing numerical results, it is important to consider the parameters which control the dependence of the P-wave NMO velocity on p. The P-wave phase velocity

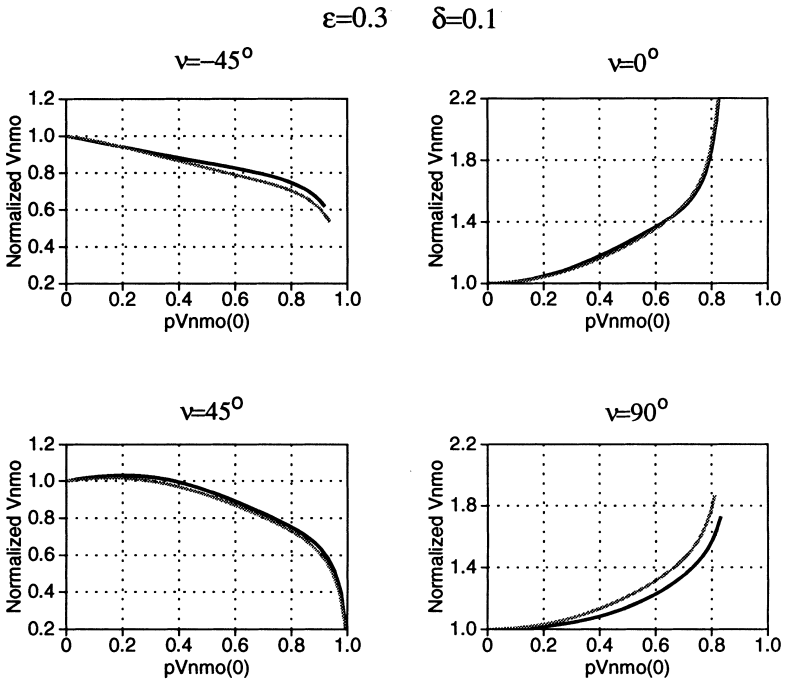

Figure 12. The influence of V_{S0} (the shear-wave velocity in the symmetry direction) on the P-wave NMO velocity. NMO velocity is computed from (4) and is normalized by (27). The curves correspond to models with $V_{P0}/V_{S0} = 1.5$ (black) and $V_{P0}/V_{S0} = 2.5$ (gray); for both models, $\epsilon = 0.3$, $\delta = 0.1$. The dips range from 0 to 70°.

can be represented as a product of the velocity in the symmetry direction (V_{P0}) and an anisotropic term dependent on the tilt ν and the anisotropic parameters ϵ and δ (the contribution of V_{S0} can be ignored). Then, according to (26), the angle ϕ can be written as

$$\phi = f(pV_{P0}, \epsilon, \delta, \nu),$$

which allows us to find the parameters of V_{nmo} from (4):

$$V_{nmo} = V_{P0} f_1(\phi, \epsilon, \delta, \nu) = V_{P0} f_2(pV_{P0}, \epsilon, \delta, \nu).$$

Therefore, the NMO velocity divided by the zero-dip value can be represented by

$$\frac{V_{nmo}(p)}{V_{nmo}(0)} = f_3(pV_{P0}, \epsilon, \delta, \nu) = f_4(pV_{nmo}(0), \epsilon, \delta, \nu). \tag{28}$$

The functions f_1, f_2, f_3, f_4 can be found explicitly by substituting the phase-velocity function into (4); however, here implicit definitions are sufficient for our purposes. Equation (28) shows that the contributions of the ray parameter and the zero-dip NMO velocity are absorbed by the term $pV_{nmo}(0)$. Essentially, changes in $V_{nmo}(0)$ (for

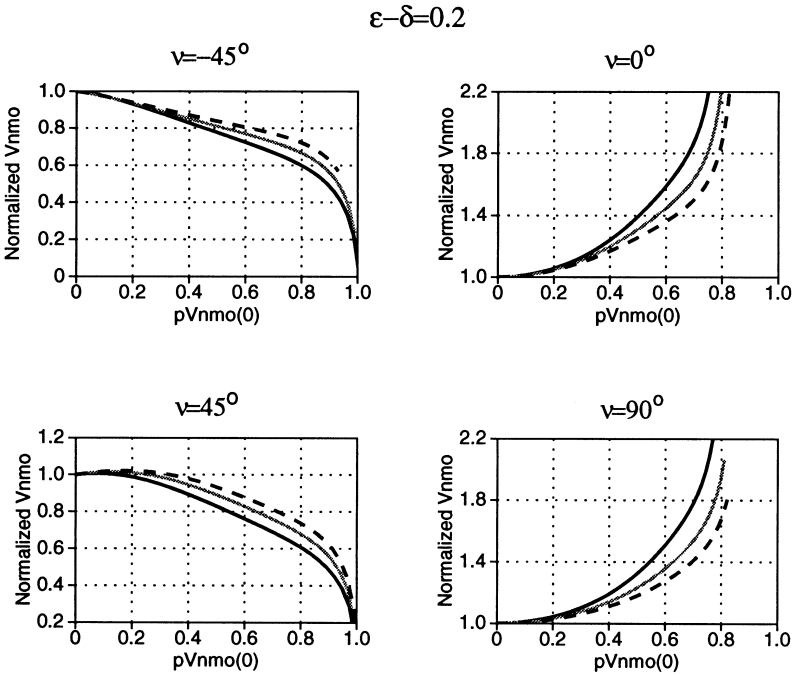

Figure 13. Normalized P-wave NMO velocity as a function of the ray parameter. The models correspond to $\epsilon - \delta = 0.2$ (as in Fig. 10): $\epsilon = 0.1$, $\delta = -0.1$ (solid black); $\epsilon = 0.2$, $\delta = 0$ (gray); $\epsilon = 0.3$, $\delta = 0.1$ (dashed). The dips range from 0 to 70°.

fixed anisotropic coefficients and tilt) just stretch or squeeze the NMO velocity curve expressed through the ray parameter. Therefore, in the calculations below $pV_{\mathrm{nmo}}(0)$ is used as the argument and the influence of the parameters ϵ, δ and ν on the NMO velocity is studied.

Since the function $V_{\mathrm{nmo}}(p)$ is of primary importance in dip-moveout (DMO) processing, in the following the dependence of the P-wave NMO velocity on the ray parameter will be called 'the DMO signature.' Hereafter, the NMO velocity is calculated from (4) as a function of $pV_{\mathrm{nmo}}(0)$ (for dips ranging from 0 to 70°) and is normalized by the isotropic expression (27) to demonstrate the distortions in the DMO signature caused by the anisotropy.

Figure 12 shows that the influence of the shear-wave velocity V_{S0} on P-wave normal moveout, ignored in (28), is indeed small. Some difference between the NMO velocities for the two models that span a wide range of $V_{\mathrm{P0}}/V_{\mathrm{S0}}$ ratios is noticeable only for a horizontal symmetry axis ($\nu = 90°$). However, this separation between the curves is caused mostly by a small influence of V_{S0} on the zero-dip NMO velocity $V_{\mathrm{nmo}}(0)$. The difference in $V_{\mathrm{nmo}}(0)$ leads to a small horizontal shift between the curves which gets amplified when the NMO velocity is divided by the isotropic equation (27) (the normalization mitigates the increase in the NMO velocity at steep dips).

The normalization by (27), equivalent to the replacement of the true dip with an 'apparent' dip angle (Larner 1993; Tsvankin 1995), leads to substantial changes in the character of the NMO curve. Note that the influence of the anisotropy on the P-wave NMO velocity becomes almost the same for vertical ($\nu = 0$) and horizontal ($\nu = 90°$) orientations of the symmetry axis, if the ray parameter is used as the argument (Fig. 13).

Comparison of Fig. 13 with Fig. 10 shows that the changes are especially pronounced for positive ν, which correspond to the symmetry axis tilted towards the reflector. For instance, at a tilt of 45° and 45° dip, the value of $pV_{\rm nmo}(0)$, which represents the sine of the apparent dip angle, is close to 0.9, which is far different from $\sin\phi \approx 0.71$. With a further increase in dip, $pV_{\rm nmo}(0)$ approaches unity (both for $\nu = 45°$ and $\nu = -45°$), and the isotropic expression (27) tends to infinity at dips well below 90° (and below $\phi_{\rm max}$ for $\nu = 45°$), leading to the sharp decrease in the normalized NMO velocity at $\nu = \pm 45°$ (Fig. 13).

Parameter η for tilted axis of symmetry

For vertical transverse isotropy, the dependence of the P-wave NMO velocity on the ray parameter is controlled by a combination of the anisotropic coefficients that Alkhalifah and Tsvankin (1995) denoted as η (equation (3)). This result makes it possible to reduce the number of parameters in DMO correction and time-related P-wave processing to just two ($V_{\rm nmo}(0)$ and η), which greatly facilitates the practical implementation of processing and inversion algorithms in VTI media. A similar result is valid for the symmetry plane of HTI media that contains the symmetry axis: in this case, the NMO velocity is governed by the parameter η of the 'equivalent' VTI medium, which is close to the generic value of η used here (Tsvankin 1997).

If the symmetry axis is tilted, the function $V_{\rm nmo}(p)$ (for the P-wave) depends on $pV_{\rm nmo}(0)$, ϵ, δ and the tilt ν (equaton (28)). The question to be addressed next is whether the influence of ϵ and δ on the NMO velocity is still absorbed by the parameter η. Note that for small δ the parameter η is close to the difference $\epsilon - \delta$, so the plots for constant $\epsilon - \delta$ given in the previous section contain a partial answer to this question. For instance, in Fig. 13 we do see some separation between the curves with the same $\epsilon - \delta$, but the general behaviour of the NMO velocity for fixed $\epsilon - \delta$ is similar. Figure 14 reproduces the result from Fig. 13, but this time the values of δ were adjusted to make $\eta = 0.2$ for all three models. Evidently, the curves moved much closer to each other, although a perfect coincidence of the NMO velocities for the full range of dips was achieved only for VTI media ($\nu = 0$). Since a detailed discussion of the signature for horizontal transverse isotropy is given in a separate paper (Tsvankin 1997), the following discussion focuses on intermediate tilt angles.

Figure 15 shows the normal-moveout velocity at the same tilt angles as in Fig. 14 but for differing values of η. While for vertical and horizontal orientations of the symmetry axis η has a pronounced influence on the NMO-velocity curves, at intermediate tilt

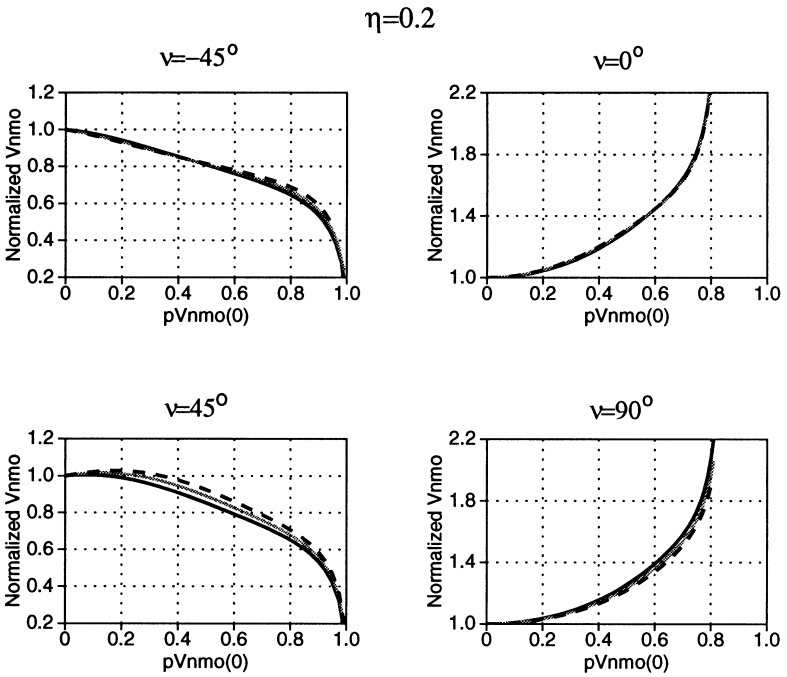

Figure 14. Normalized P-wave NMO velocity for models with the same $\eta = 0.2$: $\epsilon = 0.1$, $\delta = -0.071$ (solid black); $\epsilon = 0.2$, $\delta = 0$ (gray); $\epsilon = 0.3$, $\delta = 0.071$ (dashed). The dips range from 0 to 70°.

angles the resolution in η is considerably lower. For $\nu = \pm 45°$, the difference between the curves corresponding to $\eta = 0.2$ and $\eta = 0.3$ is relatively small (Fig. 15).

As discussed above, for weak anisotropy, deviations of the P-wave NMO velocity from the isotropic dependence (27) are proportional to the difference $\epsilon - \delta$, which is close to η for small values of δ. This is illustrated by Fig. 16, which shows that even at intermediate tilts the normalized NMO velocity still is almost linearly dependent on $\eta \approx \epsilon - \delta$ for small and moderate values of this parameter, ϵ and δ. However, with increasing η, this is no longer the case, and the curves for $\eta > 0.15$ are relatively close to each other (Figs 15 and 16).

Apparently, at $\nu = \pm 45°$ the influence of the terms quadratic in the anisotropic coefficients leads to a more complicated relationship between the NMO velocity and the parameters ϵ and δ than that in VTI media. A detailed analysis shows that the NMO velocity remains sensitive to δ as η reaches the 15–20% range, but does not change much with increasing ϵ. As a result, for $\eta = 0.15$–0.2 and higher, the DMO signature at intermediate angles depends on the individual values of ϵ and δ and is not fully controlled by η. While, for small and moderate values of η, ϵ and δ, the inversion of the NMO velocity for $\eta \approx \epsilon - \delta$ and the dip-moveout processing can be performed in the same fashion as in VTI media (provided the tilt is known), the approach developed for

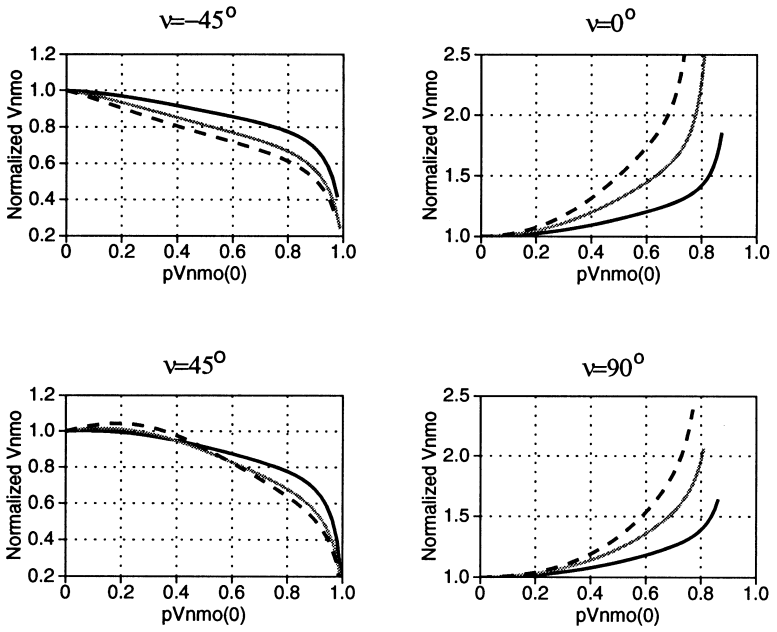

Figure 15. Normalized P-wave NMO velocity for models with different η: $\eta = 0.1$ (solid black); $\eta = 0.2$ (gray); $\eta = 0.3$ (dashed). For all models, $\delta = 0$ and $\epsilon = \eta$. The dips range from 0 to 70°.

vertical transverse isotropy cannot be used for values of η of the order of 0.15 and higher.

For completeness, Fig. 17 shows the P-wave NMO velocity at different tilt angles for (less typical) models with negative η. (If $\eta = 0$, the model is elliptical and $V_{\mathrm{nmo}}(p)$ is described by the isotropic dependence (27).) Note that at all tilts the signature for $\eta < 0$ is *reversed* compared to that for positive values of η. None the less, there is also a similarity between models with positive and negative η: in both cases, η controls the

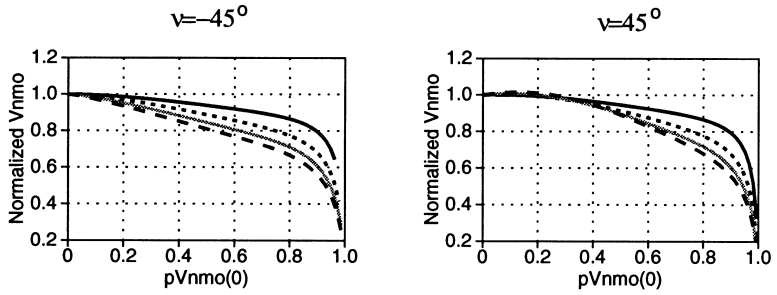

Figure 16. Sensitivity of P-wave NMO velocity to η at intermediate tilt angles. The curves correspond to $\eta = 0.05$ (solid black); $\eta = 0.1$ (dotted); $\eta = 0.15$ (gray); $\eta = 0.2$ (dashed). For all models, $\delta = 0$ and $\epsilon = \eta$. The dips range from 0 to 70°.

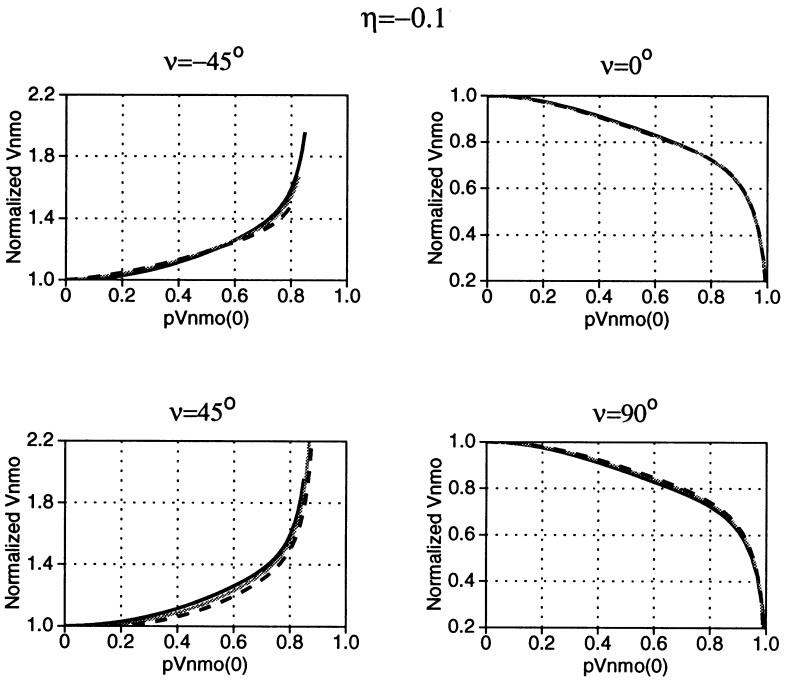

Figure 17. Normalized P-wave NMO velocity for models with $\eta = -0.1$: $\epsilon = 0$, $\delta = 0.125$ (solid black); $\epsilon = 0.1$, $\delta = 0.25$ (gray); $\epsilon = 0.2$, $\delta = 0.375$ (dashed). The dips range from 0 to 70°.

dependence $V_{\mathrm{nmo}}(p)$ more tightly for near-vertical and near-horizontal orientations of the symmetry axis than at intermediate tilt angles.

The profound differences between the dip dependence of NMO velocities for vertical transverse isotropy and TI media with a tilted axis of symmetry make it necessary to study the transition between the two signatures at mild tilt angles. Even a tilt of $\pm 20°$ is sufficient to eliminate a sharp increase in the normalized NMO velocity typical for vertical transverse isotropy and to make the DMO signature almost isotropic for a wide range of reflector dips (Figs 18 and 19). For the character of the normalized P-wave NMO velocity to be close to that in VTI media, the tilt should not exceed 10–15°. For small tilt angles within this range, the NMO velocity grows with p much faster than in isotropic media, and this increase is governed largely by η. However, it should be mentioned that even for $\nu = \pm 10°$ the anisotropic signature is less pronounced than for VTI media and the η control over the DMO signature is less tight. At tilt angles of about $\pm 30°$, the signature is reversed, and the normalized NMO velocity decreases with p.

Discussion

Transverse isotropy with a tilted axis of symmetry may be typical, for instance, for sedimentary formations near the flanks of salt domes. Here, the behaviour of

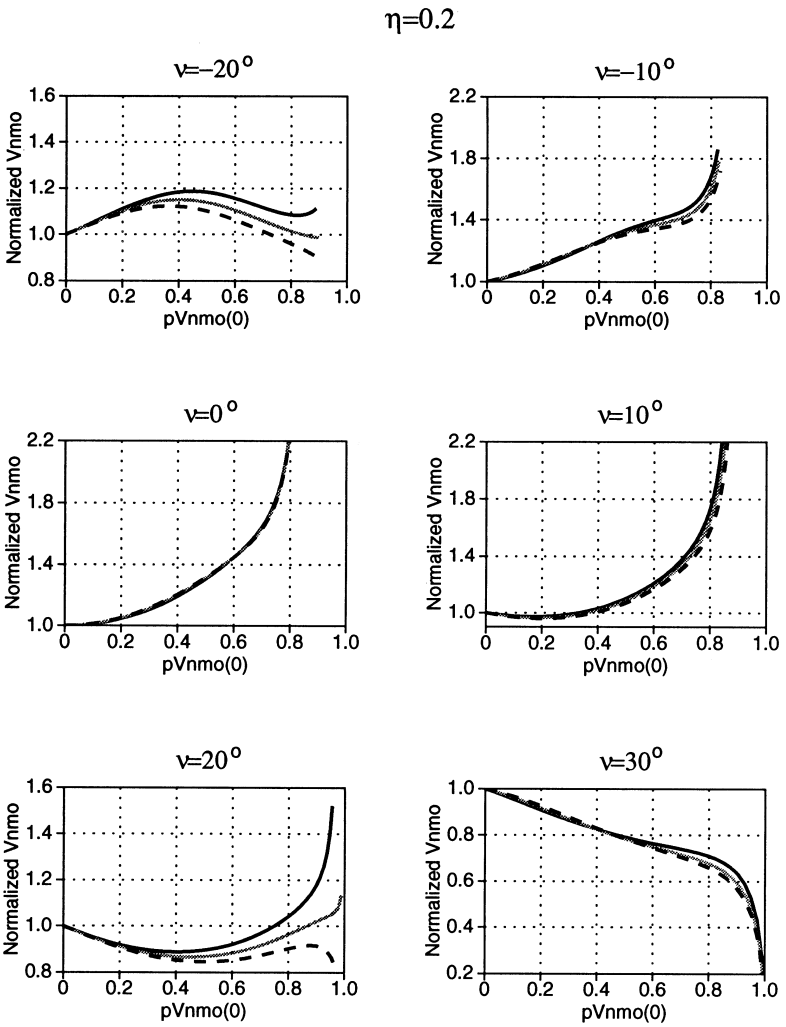

Figure 18. Normalized P-wave NMO velocity for mild tilt angles and $\eta = 0.2$: $\epsilon = 0.1$, $\delta = -0.071$ (solid black); $\epsilon = 0.2$, $\delta = 0$ (gray); $\epsilon = 0.3$, $\delta = 0.071$ (dashed). The dips range from 0 to 70°.

normal-moveout velocity was studied in the symmetry plane of TI media that contains the symmetry axis. In addition to distorting the values of NMO velocities, the influence of tilt leads to profound changes in the structure of the reflected wavefield. For homogeneous TI models with a symmetry axis tilted towards the reflector and typical values of the anisotropic parameters, it is impossible to generate specular zero-offset reflections for a certain range of steep dips that depends on the shape of the wavefront. If the medium is factorized with vertical velocity gradient, the 'missing' dips can be imaged only using turning rays, although the corresponding reflectors are sub-vertical.

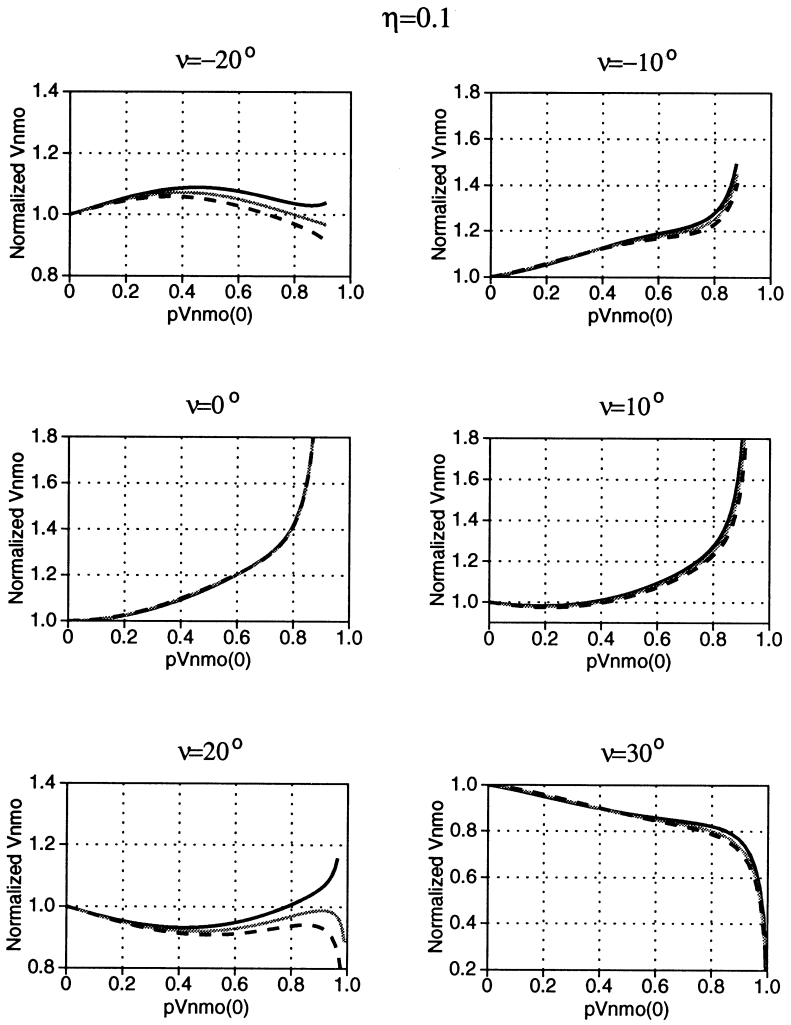

Figure 19. Normalized P-wave NMO velocity for mild tilt angles and $\eta = 0.1$: $\epsilon = 0.1$, $\delta = 0$ (solid black); $\epsilon = 0.2$, $\delta = 0.083$ (gray); $\epsilon = 0.3$, $\delta = 0.167$ (dashed). The dips range from 0 to 70°.

In a different situation, typical for the symmetry axis tilted away from the reflector, anisotropy can produce specular zero-offset reflections from overhang structures in the absence of a velocity gradient. These phenomena may cause serious complications in the imaging of such steep structures as salt domes or volcanic intrusions.

The dependence of normal-moveout velocity on the tilt angle was studied using the equation of Tsvankin (1995) valid for any strength of the anisotropy. For typical values of the anisotropic coefficients, NMO velocity provides an accurate description of reflection moveout on conventional-length spreads close to the distance between the CMP and the

reflector. For larger spreadlengths, the hyperbolic moveout equation parametrized by NMO velocity becomes inaccurate and should be replaced by more elaborate moveout approximations, such as the one suggested by Tsvankin and Thomsen (1994).

A concise approximation for NMO velocity, obtained from the exact equation in the limit of weak anisotropy, helps in understanding the influence of the tilt and anisotropic parameters on reflection moveout for all wave types. While the tilt term in the expression for the NMO velocity from horizontal reflectors is mostly determined by the difference between the Thomsen parameters ϵ and δ, the influence of tilt on the dip dependence of NMO velocity has a more complicated character.

For purposes of seismic inversion and processing, NMO velocity from dipping reflectors should be studied as a function of the ray parameter p (the dependence $V_{\rm nmo}(p)$ is called here the 'dip-moveout (DMO) signature'). If the medium is elliptically anisotropic ($\epsilon = \delta$) with tilted elliptical axes, the dependence $V_{\rm nmo}(p)$ is shown to be described by the same equation as in isotropic media. Since the reflection moveout in elliptical media is purely hyperbolic, all isotropic time-related processing methods (NMO, DMO, time migration) are entirely valid for elliptical anisotropy with any orientation of the elliptical axes. Time-to-depth conversion, however, requires knowledge of the vertical velocity, which cannot be found from moveout data alone. It should be mentioned that the NMO velocity from horizontal reflectors in elliptical models remains close to the horizontal phase velocity.

For vertical transverse isotropy, the P-wave DMO signature is tightly controlled by just two effective parameters: the zero-dip NMO velocity $V_{\rm nmo}(0)$ and the anellipticity coefficient η. The same two parameters determine the time-migration impulse response and, therefore, are sufficient for all time-related processing methods in VTI media (Alkhalifah and Tsvankin 1995). The numerical results for TI media with a tilted symmetry axis show that for relatively small values of ϵ and δ, the P-wave DMO signature depends only on η and the tilt angle. However, due to the influence of the higher-order anisotropic terms at intermediate tilt angles, this conclusion does not hold if the coefficients ϵ, δ or η exceed 10–15%.

On the whole, the dependence of the NMO velocity on the ray parameter has the same character as for vertical transverse isotropy only for a narrow range of tilt angles corresponding to near-vertical and near-horizontal orientations of the symmetry axis. For horizontal transverse isotropy, the NMO velocity is controlled by the parameter η of the 'equivalent' VTI medium, which is relatively close to the generic value of η (Tsvankin 1997). For mild tilts away from the vertical, the behaviour of the P-wave NMO velocity is similar to that in VTI media: for typical $\eta > 0$, $V_{\rm nmo}$ increases with p much faster than in isotropic (or elliptically anisotropic) media and is tightly controlled by η (at a fixed tilt ν). However, the comfortable limit for applying the approaches developed for VTI media is only about $\nu = \pm 10°$. A tilt of $\pm 20°$ is sufficient to eliminate the anisotropic DMO signature almost entirely and to make the NMO velocity much less dependent on η. At larger tilts of $\pm(30–55)°$, the signature is reversed, with $V_{\rm nmo}(p)$ increasing more slowly than in isotropic media and being controlled by η only for small and moderate values of this parameter ($|\eta| \leq 0.15 - 0.2$), ϵ and δ.

Provided that the tilt angle is known, the dependence $V_{\mathrm{nmo}}(p)$ can be reliably inverted for η only when the symmetry axis is close either to the vertical or to the horizontal. Also, η can be obtained in the $\pm$ (30–55)° tilt range, but only for small values of the anisotropic parameters. An interesting implication of the above results is the possibility of using the DMO signature in the inversion for the orientation of the symmetry axis. In general, this inversion would require a 3D azimuthal analysis of reflection traveltimes on survey lines with different directions. However, if the plane containing the symmetry axis has been identified, the strong dependence of the P-wave NMO velocity on the tilt angle can sometimes be used to constrain the tilt. For instance, if the formation has a known value of η (say, a typical positive value for shales), the disappearance of the anisotropic DMO signature is indicative of a tilt of about $\pm 20°$. If the signature is reversed (i.e. the normalized NMO velocity decreases with p), we can conclude that the tilt should be of the order of $\pm 30°$ or more. Note, however, that the influence of the anisotropy on the P-wave function $V_{\mathrm{nmo}}(p)$ can also be reduced by a positive vertical-velocity gradient (Larner 1993; Tsvankin 1995). Hence, the estimation of the tilt angle would be impossible without properly accounting for vertical inhomogeneity.

The substantial magnitude of deviations of the P-wave DMO signature from the isotropic one in several ranges of tilt angles means that conventional isotropic DMO cannot be applied to many typical transversely isotropic models. Some existing anisotropic dip-moveout algorithms based on the exact NMO velocity equation (4) (e.g. the Hale-type DMO method of Anderson and Tsvankin 1994) can be directly used in the symmetry plane of TI media with a tilted symmetry axis. The main problem in the application of anisotropic DMO to TI media with a tilted axis of symmetry is the estimation of the anisotropic parameters. Although the DMO signature is not fully controlled by η and the tilt may not be exactly known, it may still be possible to find an 'effective' transversely isotropic model with the correct dependence $V_{\mathrm{nmo}}(p)$ for the available dipping events. The anisotropic parameters and the tilt angle provide extra degrees of freedom in the NMO equation, thus making this approach feasible. However, the parameters recovered from the fitting procedure would represent just one possible anisotropic model, which would be suitable for DMO processing but not necessarily for poststack migration or estimation of the actual anisotropic coefficients.

Although the above analysis was performed for a single transversely isotropic layer, the results can be extended to vertically inhomogeneous media by using the generalized Dix equation of Alkhalifah and Tsvankin (1995). This equation is valid in symmetry planes of any anisotropic model that consists of a dipping reflector beneath a vertically stratified overburden. Each layer, for instance, can be transversely isotropic with an in-plane symmetry axis tilted at an arbitrary angle. The NMO velocity for such a model is represented by an rms average of the single-layer NMO velocities that were discussed in this paper.

Conclusions

The results listed below were obtained for the vertical symmetry plane containing the symmetry axis of the transversely isotropic model and the reflector normal.

1. For typical homogeneous TI models, tilt of the symmetry axis towards the reflector leads to the disappearance of specular reflections from steep interfaces.
2. In the presence of vertical velocity gradient, the 'missing' sub-vertical dipping planes do generate specular reflections, which in this case represent turning rays. These phenomena can cause serious problems in salt imaging, even if the processing algorithms take the influence of transverse isotropy into account.
3. On conventional-length spreads close to the distance between the CMP and the reflector, P-wave moveout is sufficiently close to a hyperbola parametrized by NMO velocity.
4. For elliptically anisotropic media with *any* tilt of the symmetry axis, the dependence of the NMO velocity on the ray parameter $V_{\rm nmo}(p)$ ('the DMO signature') is exactly the same as in isotropic media. All isotropic time-related processing methods (NMO, DMO, time migration) are entirely valid in elliptical media.
5. In non-elliptical TI media, the function $V_{\rm nmo}(p)$ for P-waves is similar to the one for vertical transverse isotropy *only* for near-vertical and near-horizontal orientations of the symmetry axis. A tilt of about 20° is sufficient to eliminate the influence of anisotropy on the DMO signature (but not on the zero-dip NMO velocity $V_{\rm nmo}(0)$). At larger tilt angles, $V_{\rm nmo}(p)$ normalized by the corresponding isotropic function is *reversed* compared to the NMO curve for vertical transverse isotropy.
6. The P-wave DMO signature is controlled by the tilt of the symmetry axis and the anisotropic parameters ϵ and δ, with the difference $\epsilon - \delta$ responsible for the character of deviations from the isotropic dependence $V_{\rm nmo}(p)$. However, in contrast to VTI media, the influence of ϵ and δ at intermediate tilt angles is *not* fully absorbed by the parameter $\eta = (\epsilon - \delta)/(1 + 2\delta)$, unless anisotropy is weak.
7. Conventional isotropic DMO correction is not suitable for a wide range of tilt angles and should be replaced with algorithms honouring the influence of transverse isotropy on NMO velocity.

Acknowledgements

I thank members of the 'A(anisotropy)-Team' at the Center for Wave Phenomena (CWP), Colorado School of Mines, for useful discussions. I am grateful to Jack Cohen and Ken Larner for their reviews of the manuscript and to Vladimir Grechka and Andreas Rüger (all of CWP) for use of their anisotropic ray-tracing codes. The support for this work was provided by the members of the Consortium Project on Seismic Inverse Methods for Complex Structures at CWP, and by the United States Department of Energy (project "Velocity Analysis, Parameter Estimation, and Constraints on Lithology for Transversely Isotropic Sediments" within the framework of the Advanced Computational Technology Initiative).

Appendix A
NMO velocity for elliptically anisotropic media

Here, normal-moveout velocity for elliptically anisotropic media with tilted in-plane

elliptical axes is obtained from (4). To satisfy the assumptions behind (4), we also assume the incidence plane to be the dip plane of the reflector.

For elliptical anisotropy, P-waves are described by a single anisotropic parameter δ ($\epsilon = \delta$). If the symmetry axis makes an angle ν with the vertical, the P-wave phase-velocity function is given by

$$V_{\mathrm{P}}(\theta) = V_{\mathrm{P0}}\sqrt{1 + 2\delta \sin^2 \bar{\theta}}, \tag{A1}$$

where $\bar{\theta} = \theta - \nu$, V_{P0} is the P-wave phase and group velocity along the symmetry axis. Note that both θ and ν may be either positive or negative; we will assume that the positive direction is counterclockwise from the vertical axis that points downwards.

The derivatives of the phase velocity needed to evaluate the NMO velocity (4) are obtained from (A1) as

$$V'_{\mathrm{P}}(\theta) = \frac{V_{\mathrm{P0}}\delta \sin 2\bar{\theta}}{(1 + 2\delta \sin^2 \bar{\theta})^{1/2}}, \tag{A2}$$

$$V''_{\mathrm{P}}(\theta) = 2V_{\mathrm{P0}}\delta \frac{\cos 2\bar{\theta} - 2\delta \sin^4 \bar{\theta}}{(1 + 2\delta \sin^2 \bar{\theta})^{3/2}}. \tag{A3}$$

Substituting (A1)–(A3) into (4) yields

$$V_{\mathrm{nmo}}(\phi) = \frac{V_{\mathrm{P0}}}{\cos \phi}\sqrt{1 + 2\delta}\sqrt{1 + 2\delta \sin^2(\phi - \nu)}\left[1 - 2\delta \frac{\sin \nu \sin(\phi - \nu)}{\cos \phi}\right]^{-1}. \tag{A4}$$

Next, let us express the NMO velocity as a function of the ray parameter p. The function $V_{\mathrm{nmo}}(p)$ for elliptical anisotropy with a vertical symmetry axis has the same form as in isotropic media (Tsvankin 1995; Alkhalifah and Tsvankin 1995):

$$V_{\mathrm{nmo}}(p) = \frac{V_{\mathrm{nmo}}(0)}{\sqrt{1 - p^2 V^2_{\mathrm{nmo}}(0)}}, \tag{A5}$$

with

$$V_{\mathrm{nmo}}(0) = V_{\mathrm{P0}}\sqrt{1 + 2\delta}.$$

Here, we will prove that the isotropic relationship (A5) holds in elliptically anisotropic media irrespective of the tilt of the elliptical axes. It is easier to carry out this proof by transforming (A5) into (A4) rather than the other way around.

Using (A1), we represent the ray parameter as

$$p = \frac{\sin \phi}{V(\phi)} = \frac{\sin \phi}{V_{\mathrm{P0}}\sqrt{1 + 2\delta \sin^2(\phi - \theta)}}. \tag{A6}$$

The zero-dip NMO velocity $V_{\mathrm{nmo}}(0)$ for arbitrary tilt of the symmetry axis can be found from (A4):

$$V_{\mathrm{nmo}}(0) = \frac{V_{\mathrm{P0}}\sqrt{1 + 2\delta}}{\sqrt{1 + 2\delta \sin^2 \nu}}. \tag{A7}$$

Substituting (A6) and (A7) into the isotropic equation (A5) for $V_{\rm nmo}(p)$, we get

$$V_{\rm nmo}(\phi) = \frac{V_{\rm P0}\sqrt{1+2\delta}\sqrt{1+2\delta\sin^2(\phi-\nu)}}{d}, \tag{A8}$$

where $d = \{1+2\delta[\sin^2\nu + \sin^2(\phi-\nu)] + 4\delta^2\sin^2\nu\sin^2(\phi-\nu) - (1+2\delta)\sin^2\phi\}^{1/2}$.

The denominator d can be simplified further to

$$d = \cos\phi - 2\delta\sin\nu\sin(\phi-\nu),$$

and (A8) reduces to (A4).

Appendix B
Weak-anisotropy approximation for NMO velocity

For weak transverse isotropy ($|\epsilon| \ll 1, |\delta| \ll 1, |\gamma| \ll 1$), the NMO equation (4) can be significantly simplified by retaining only the terms linear in the anisotropic coefficients ϵ, δ (for the P- and SV-waves), and γ (for the SH-wave). First, we expand (4) in the anisotropic terms $[V''(\phi)/V(\phi)]$ and $[\tan\phi V'(\phi)/V(\phi)]$, which turn to zero in isotropic media. Dropping the quadratic and higher-order terms in this expansion, we get

$$V_{\rm nmo}(\phi) = \frac{V(\phi)}{\cos\phi}\left[1 + \frac{V''(\phi)}{2V(\phi)} + \tan\phi\frac{V'(\phi)}{V(\phi)}\right]. \tag{B1}$$

For P-waves, the phase-velocity function, fully linearized in the anisotropic coefficients ϵ and δ, was given by Thomsen (1986). In the case of the symmetry axis tilted at an angle ν from the vertical, the weak-anisotropy approximation for the phase velocity becomes

$$V_{\rm P}(\theta) = V_{\rm P0}(1 + \delta\sin^2\bar{\theta}\cos^2\bar{\theta} + \epsilon\sin^4\bar{\theta}), \tag{B2}$$

where $\bar{\theta} = \theta - \nu$.

The derivatives of $V_{\rm P}$ (B2) to be used in (4) are

$$V'(\theta) = V_{\rm P0}\sin 2\bar{\theta}(\delta\cos 2\bar{\theta} + 2\epsilon\sin^2\bar{\theta}), \tag{B3}$$

$$V''(\theta) = 2V_{\rm P0}[\delta\cos 4\bar{\theta} + 2\epsilon\sin^2\bar{\theta}(1+2\cos 2\bar{\theta})]. \tag{B4}$$

Since the phase velocity and its derivatives (B2)–(B4) should be evaluated at the angle $\theta = \phi$, they become functions of the variable $\bar{\phi} = \phi - \nu$. It is convenient to rewrite (B1) as

$$V_{\rm nmo}(\phi)\cos\phi = V(\bar{\phi})\left[1 + \frac{V''(\bar{\phi})}{2V(\bar{\phi})} + \tan\bar{\phi}\frac{V'(\bar{\phi})}{V(\bar{\phi})} + (\tan\phi - \tan\bar{\phi})\frac{V'(\bar{\phi})}{V(\bar{\phi})}\right]. \tag{B5}$$

The term

$$C(\bar{\phi}) = V(\bar{\phi})\left[1 + \frac{V''(\bar{\phi})}{2V(\bar{\phi})} + \tan\bar{\phi}\frac{V'(\bar{\phi})}{V(\bar{\phi})}\right] \tag{B6}$$

has exactly the same form as $[V_{\rm nmo}(\phi)\cos(\phi)]$ for a vertical axis of symmetry

($\nu = 0, \bar{\phi} = \phi$). The weak-anisotropy approximation for VTI media was obtained by Tsvankin (1995):

$$V_{\rm nmo}(\phi)\cos\phi = V_{\rm P0}[1 + \delta + \delta\sin^2\phi + 3(\epsilon - \delta)\sin^2\phi(2 - \sin^2\phi)]. \tag{B7}$$

Replacing ϕ with $\bar{\phi}$ in (B7) allows us to represent $C(\bar{\phi})$ from (B6) as

$$C(\bar{\phi}) = V_{\rm P0}[1 + \delta + \delta\sin^2\bar{\phi} + 3(\epsilon - \delta)\sin^2\bar{\phi}(2 - \sin^2\bar{\phi})]. \tag{B8}$$

Using (B2) and (B3), we find the weak-anisotropy approximation for the remaining term in (B5):

$$(\tan\phi - \tan\bar{\phi})\frac{V'(\bar{\phi})}{V(\bar{\phi})} = \frac{2\sin\nu\sin\bar{\phi}}{\cos\phi}[\delta + 2(\epsilon - \delta)\sin^2\bar{\phi}]. \tag{B9}$$

Substituting (B8) and (B9) into (B5) yields

$$V_{\rm nmo}(\phi)\cos\phi = V_{\rm P0}\left\{1 + \delta + \delta\sin^2\bar{\phi} + 3(\epsilon - \delta)\sin^2\bar{\phi}(2 - \sin^2\bar{\phi}) + \frac{2\sin\nu\sin\bar{\phi}}{\cos\phi}[\delta + 2(\epsilon - \delta)\sin^2\bar{\phi}]\right\}. \tag{B10}$$

Equation (B10) is the weak-anisotropy approximation for the P-wave NMO velocity fully linearized in the anisotropic parameters ϵ and δ.

References

Alkhalifah T. and Tsvankin I. 1995. Velocity analysis for transversely isotropic media. *Geophysics* **60**, 1550–1566.

Anderson J. and Tsvankin I. 1994. Dip-moveout processing by Fourier transform in anisotropic media. 64th SEG meeting, Los Angeles, Expanded Abstracts, 1213–1216.

Banik N.C. 1984. Velocity anisotropy of shales and depth estimation in the North Sea basin. *Geophysics* **49**, 1411–1419.

Berryman J.G. 1979. Long-wave elastic anisotropy in transversely isotropic media. *Geophysics* **44**, 896–917.

Byun B. 1982. Seismic parameters for media with elliptical velocity dependencies. *Geophysics* **47**, 1621–1626.

Dix C. H. 1955. Seismic velocities from surface measurements.*Geophysics* **20**, 68–86.

Hake H., Helbig K. and Mesdag C. S. 1984. Three-term Taylor series for $t^2 - x^2$curves over layered transversely isotropic ground. *Geophysical Prospecting* **32**, 828–850.

Helbig K. 1983. Elliptical anisotropy–its significance and meaning.*Geophysics* **48**, 825–832.

Larner K. 1993. Dip-moveout error in transversely isotropic media with linear velocity variation in depth. *Geophysics* **58**, 1442–1453.

Levin F.K. 1971. Apparent velocity from dipping interface reflections. *Geophysics* **36**, 510–516.

Levin F.K. 1979. Seismic velocities in transversely isotropic media. *Geophysics* **44**, 918–936.

Levin F.K. 1990. Reflection from a dipping plane–Transversely isotropic solid. *Geophysics* **55**, 851–855.

Lyakhovitsky F. and Nevsky M. 1971. The traveltime curves of reflected waves in a transversely isotropic medium. *Dokl. Acad. Nauk SSSR* **196**, 327–330 (in Russian).

Rüger A. and Alkhalifah T. 1996. Efficient two-dimensional anisotropic ray tracing. In: *Proceedings of the 6th International Workshop on Seismic Anisotropy*, SEG Tulsa, 556–600.

Sayers C.M. 1994. The elastic anisotropy of shales. *Journal of Geophysical Research* **99**, No. B1, 767–774.

Sena A.G. 1991. Seismic traveltime equations for azimuthally anisotropic and isotropic media: Estimation of interval elastic properties. *Geophysics* **56**, 2090–2101.

Seriff A.J. and Sriram K.P. 1991. *P–SV* reflection moveouts for transversely isotropic media with a vertical symmetry axis. *Geophysics* **56**, 1271–1274.

Taner M.T. and Koehler F. 1969. Velocity spectra – digital computer derivation and application of velocity functions. *Geophysics* **34**, 859–881.

Thomsen L. 1986. Weak elastic anisotropy. *Geophysics* **51**, 1954–1966.

Thomsen L. 1988. Reflection seismology over azimuthally anisotropic media. *Geophysics* **53**, 304–313.

Thomsen L. 1995. Elastic anisotropy due to aligned cracks in porous rock. *Geophysical Prospecting* **43**, 805–830.

Tsvankin I. 1995. Normal moveout from dipping reflectors in anisotropic media. *Geophysics* **60**, 268–284.

Tsvankin I. 1996. *P*-wave signatures and notation for transversely isotropic media: An overview. *Geophysics* **61**, 467–483.

Tsvankin I. 1997. Reflection moveout and parameter estimation for horizontal transverse isotropy. *Geophysics*, **62**, 614–629.

Tsvankin I. and Thomsen L. 1994. Nonhyperbolic reflection moveout in anisotropic media. *Geophysics* **59**, 1290–1304.

Uren N.F., Gardner G.N.F. and McDonald J.A. 1990. Normal moveout in anisotropic media. *Geophysics* **55**, 1634–1636.